POAC'23
Glasgow, United Kingdom

Proceedings of the 27th International Conference on
Port and Ocean Engineering under Arctic Conditions
12-16 June 2023, Glasgow, United Kingdom

Ice Conditions in Beisfjord, Norway from 2021 – 2023

Megan O'Sadnick[1], Chris Petrich[1]
[1] SINTEF Narvik, Narvik, Norway

ABSTRACT

Since 2017, observations of ice conditions have been made in the northern Norwegian fjord, Beisfjord, to better understand the mechanisms of ice formation and variability in ice thickness, crystallography, and properties including salinity and $\delta^{18}O$. Data from Fall 2017 to Spring 2020 have previously been presented, here we provide results from Fall 2021 through Spring 2023. Ice formed late November for both the 2021 – 22 and 2022 - 23 season but weather conditions, namely the freezing degree days from formation to measurement, differed significantly, 314 versus 132 ° C days respectively, with the latter season being considerably warmer in the first two to three months of ice cover. The ice cores gathered between the two seasons showed similarities including low bulk salinity values, being all below 2 ppt, as well as $\delta^{18}O$ being consistently below -8‰. Five out of the six cores gathered over the two season also had a considerable layer of both granular and congelation ice. Where samples differ is in their total thickness with the three cores from the first season averaging 25 cm while in the second season cores were slightly thicker, on average 30 cm, despite fewer freezing degree days. Additionally, cores gathered in 2022 - 23 also showed less variation between the cores gathered. The reasons for these differences are thought to be related to ice extent and snow and oceanic heat.

KEY WORDS: Fjord ice; Sea ice; Coastal processes; Norway

INTRODUCTION

From 2017 – 2020, observations and measurements of ice conditions and properties were gathered in seven fjords located in northern Norway. Results presented by O'Sadnick et al. (2022) show clear evidence of decoupling of a fresh or brackish surface layer and the warmer, saltier intermediary layer below at the time of freezing. A significant amount of variation was present, however, not only in ice properties but ice thickness, extent, and stratigraphy. Freezing degree days were shown to be poor predictor of ice thickness with the timing of different weather and oceanic conditions including air temperature, snowfall, tides, wind, and runoff all likely having an influence. Given a lack of long-term observations of fjord ice, the measurement campaign has continued in the furthest south fjord, Beisfjord located at 68°23.6′ N, 17°30.5′ E (Fig. 1). Here we present findings from the 2021 – 22 and 2022 – 23 winter seasons.

Beisfjord is a relatively small sill fjord being 8 km in length, and 0.8-1.0 km wide with a maximum depth of 44 m and a sill depth of on 3 – 4 m at its mouth. At the head of the fjord is Lakselva drainage basin, having a catchment area of 159 km^2 and an annual inflow, the amount of water that flows into the catchment, of over 222 million m^3/year (Norges Vassdrags- og Energidirektorat, 2019). While most of this inflow comes in the spring through

the summer, the river has been observed to flow throughout the winter despite substantial freeze-up in lakes and tributaries of the river. As freshwater enters the fjord during the wintertime, it will create a stratified water column when surface mixing is limited (e.g. due to little wind). Cooling of this upper layer can occur quickly leading to thin layers of ice to form (O'Sadnick,2022; Kvambekk, 2010, Asvall 2010). If conditions persist, this ice will further thicken through either growth downward (congelation ice) or upward through the formation of granular snow ice or superimposed ice. In the following, ice cores are examined in line with measurements of bulk ice salinity and $\delta^{18}O$ to determine the distribution of congelation and granular ice and, relatedly, gain understanding of the processes that led to ice formation and growth. Weather conditions while ice was present are next examined to provide further context for findings from the ice core analysis and determine how they may be connected to variations in ice extent.

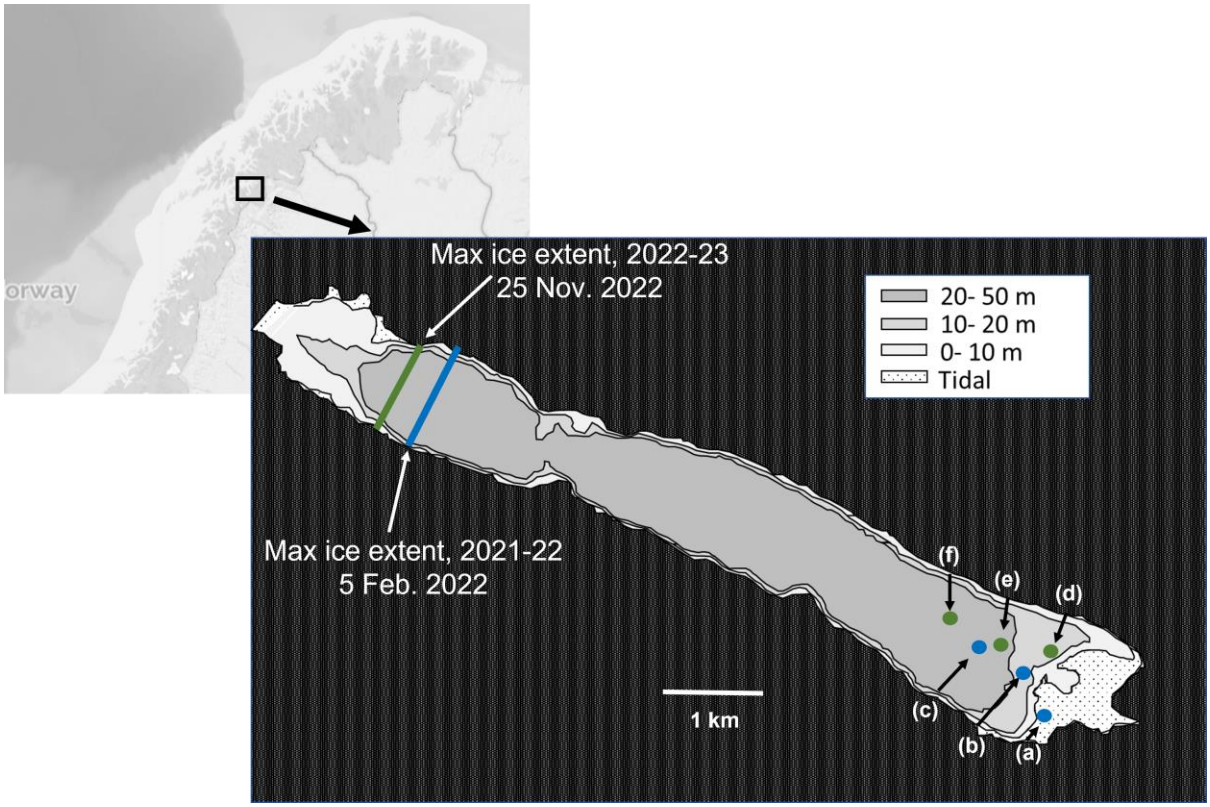

Figure 1. Map of Beisfjord with water depths marked. Maximum ice extent and position of each core with 2021 – 22 shown in blue and 2022 – 23 shown in green. Letter associated with each core aligns with Fig.2.

METHODS

Field Measurements

For a complete description of the field methods, external measurements and weather data, please see O'Sadnick et al. (2022). All ice samples were gathered after removing snow from the ice area. At least two cores were next taken with one being sliced into approximately 0.05 m thick sections for subsequent melting and measurement of bulk salinity and $\delta^{18}O$ and the second kept intact for vertical slicing and analysis of stratigraphy. To measure bulk ice salinity of melted samples, a YSI Pro30 temperature/conductivity probe was used, having an accuracy of 0.1 on the practical salinity scale (psu) (Fofonoff & Millard, 1983) and resolution of ±0.1 (psu) or ±1% of the reading, whichever is greater. The remaining seawater from the

melted ice samples was placed in glass bottles with cone liners and stored at 4 °C for stable oxygen isotope analysis. Samples were analyzed at the Stable Isotope Laboratory at the Centre for Arctic Gas Hydrate, Environment and Climate (CAGE) located at UiT The Arctic University of Norway, Tromsø, Norway. The remaining core was stored at -18 °C to ensure minimal brine drainage before being sliced vertically in a cold room set to approximately -12 °C. Ice type and transitions were next examined and photographed by sandwiching the vertical thick section between cross-polarized filters.

Measurements of ocean salinity and temperature were made with the same temperature/conductivity probe described above lowered to a depth of approximately 1 m below the ice/ocean interface. Ocean water samples were also obtained by lowering a tube to a similar depth (marked in Table 1), releasing the pressure to allow water to flow into the tube before re-plugging and bringing to the surface. Additionally, freshwater river samples were gathered from the same location as those gathered in previous years. Both ocean and river samples were sent alongside ice samples for measurement of $\delta^{18}O$.

External Measurements

A UOVision UM 565 trail camera positioned at 68°22.1′ N, 17°38.0′ E and elevation of 390 m was used to collect time-lapse images of Beisfjord. This allowed for tracking of weather events and determination of ice freeze up and break up. As the camera became blocked by the snow on the lens sporadically through the winter season, satellite imagery was also used to track ice conditions. For this purpose, the SENTINEL-1 C-band Synthetic Aperture Radar (SAR) scenes were evaluated after processing in Google Earth Engine (Gorelick et al., 2017). Here, freeze up is defined as the first day of consistent ice coverage and break up as the first day with no ice present in the fjord. The ice season is defined as the period between first freeze up and last break up.

Weather Data

Values for average daily air temperature, accumulated snow cover, and rainfall plus snowmelt were obtained from the openly available web portal seNorge.no (Lussana et al., 2018), providing spatially interpolated observational data from the Norwegian Meteorological Institute and the Norwegian Water Resources and Energy Directorate (NVE). Temperature data was analyzed to calculate freezing degree days (FDD) between the date of freeze up to the date of measurement. FDDs are derived by summing all average daily air temperatures (T_a) below freezing point (T_f) from the start date (i=1, date of freeze-up) to end date (i=N, date of measurement):

$$FDD = \sum_{i=1}^{N} \Delta t \begin{cases} T_f - T_{a,i}, & T_{a,i} < T_f \\ 0, & T_{a,i} \geq T_f \end{cases} \quad (1)$$

where Δt= 1 day.

Freezing degree days can be used in the prediction of thermodynamic ice growth and resultant thickness such as described by Anderson (1961) through the equation:

$$H^2 + 5.1H = 6.7\theta \quad (2)$$

where H is ice thickness in cm and θ is freezing degree days in °C days.

In the following, the freezing temperature of freshwater (T_f = 0 °C) is used to calculate FDD and ice thickness due to bulk ice salinity and $\delta^{18}O$ indicating a large fraction of freshwater in this boundary layer (cf. Results and Discussion). Variability in salinity of water at the interface and thus the freezing point is expected with higher salinities leading to lower freezing points and therefore lower values of FDD and predicted ice thickness. The results

presented here can here can thus be considered upper limits. Further discussion of the impact freezing temperature can be found in O'Sadnick et al. (2022) and O'Sadnick et al. (2023).

RESULTS AND DISCUSSION

Ice properties and type

Thick sections aligned with salinity and $\delta^{18}O$ profiles are presented in Fig. 2a and 2b for 2021/22 and 2022/23, respectively. The cores all display bulk salinity values below 2 psu, often below 1 psu, while $\delta^{18}O$ was consistently below -8 ‰. Granular ice composes a considerable fraction of all but core (c). The transition from granular to congelation ice, clear in cross-polarized images, is marked by an increase of 1 ‰ in the $\delta^{18}O$ profiles (except core (e) of 2022/23). Bulk ice salinity is continuously below 0.25 psu across the two types of ice in 2021/22, while it drops by approx. 0.5 psu from ca 1 psu in 2022/23. The minimal contrast between the two ice types in the samples shown here can be better understood by deriving the composition of water at the ice – ocean interface during ice growth using the method provided in O'Sadnick et al. (2023). Results show that samples of congelation ice were all grown from water > 92 % freshwater (equivalent to a salinity < 2.4 psu). From observation of weather conditions (detailed further below), granular ice can be assumed to be derived from snow having a salinity of 0 psu and $\delta^{18}O$ of < 11 ‰ (based on previous measurements presented in O'Sadnick et al. (2022)) thus the two ice types, although different in their origin, are similar in freshwater content. On the day ice samples were collected, water 1 m under ice measured above 31.4 psu and – 1.5 ‰ indicating that the freshwater at the interface during ice growth was temporary and/or existed as a thin, unmixed layer at the ice – ocean interface.

Table 1. Summary of ice conditions at each core location.

Core	Freeze - up	Date of meas.	Break - up	FDD (°C days) to meas.	Predicted thickness (cm)	Total thickness (cm)	Thickness of congelation ice (cm)	Ocean Salinity (psu)	Ocean Temp (°C)	$\delta^{18}O$, ocean (‰)	$\delta^{18}O$, river (‰)
a	28 Nov. 2021	7 Feb. 2022	13 Apr. 2022	314	43	25	6	31.6	3.6	not tested	-11,7
b				314	43	32	17	31.5	4.5	-1.5 (1 m)	
c	approx. 27 Jan. 2022			60	18	19	19	31.4	4.4	not tested	
d	25 Nov. 2022	11 Jan. 2023	23 Apr. 2023	132	27	31	14	31.7	6.1	-0.9 (1.2 m)	-12.1
e				132	27	31	9	32	6.1	not tested	
f				132	27	29	15	32.1	6.2	not tested	

Table 1 provides a summary of freeze-up dates, freezing degree days, ice thickness, and ocean and river data. The three cores gathered during the 2021 – 2022 season (a-c) show a greater variation in thickness and type of ice. Core (b), was thickest having 15 cm of granular snow ice and approximately 17 cm of congelation ice. Core (a) was only 25 cm and composed of more snow ice (20 cm) and only approximately 6 cm of congelation ice. The last core of 19 cm was composed entirely of congelation ice. The variety in these cores is representative of the changing weather conditions (e.g. snowfall, melt, wind transport of snow) and variation in ice extent through the season. As shown in Fig. 3, ice extent continuously decreased in the first two months of the ice season before more ice formed at the beginning of February, reaching a maximum ice extent on 5 February shortly before ice samples were taken. Through analysis of timelapse imagery it was found that core (c) formed approximately two months after cores (a) and (b) leading to the former experiencing only 60 FDDs in comparison to 314 FDDs for the latter two on the day of measurement. Cores (a) and (b) are significantly thinner than what is predicted from Eq. 2, however, with or without incorporating granular snow ice. While varying the value for $T_{f,}$ will decrease this difference slightly, three main factors are assumed to have a much greater impact - above-melting temperatures, insulation by snow and oceanic heat flux. All factors will alter heat flux

through the ice, limiting growth of ice downwards and potentially leading to melt at the ice-ocean interface. Core (c) shows good agreement with results from Eq. 2. No snow was on the surface when the core was taken, thus this last core formed without any insulation by snow that could have slowed growth. Additionally, given only approximately two weeks from formation to measurement, less time was available for melt from the ice-ocean interface to occur, and there were no periods of above-freezing temperatures. In contrast, cores (a) and (b) were 17 cm thinner than predicted. This can be explained by a combination of several periods of above-freezing air temperatures, thermal insulation from a snow cover, and potentially bottom melt from oceanic heat. The former two were directly observed during the two months leading up to the measurements.

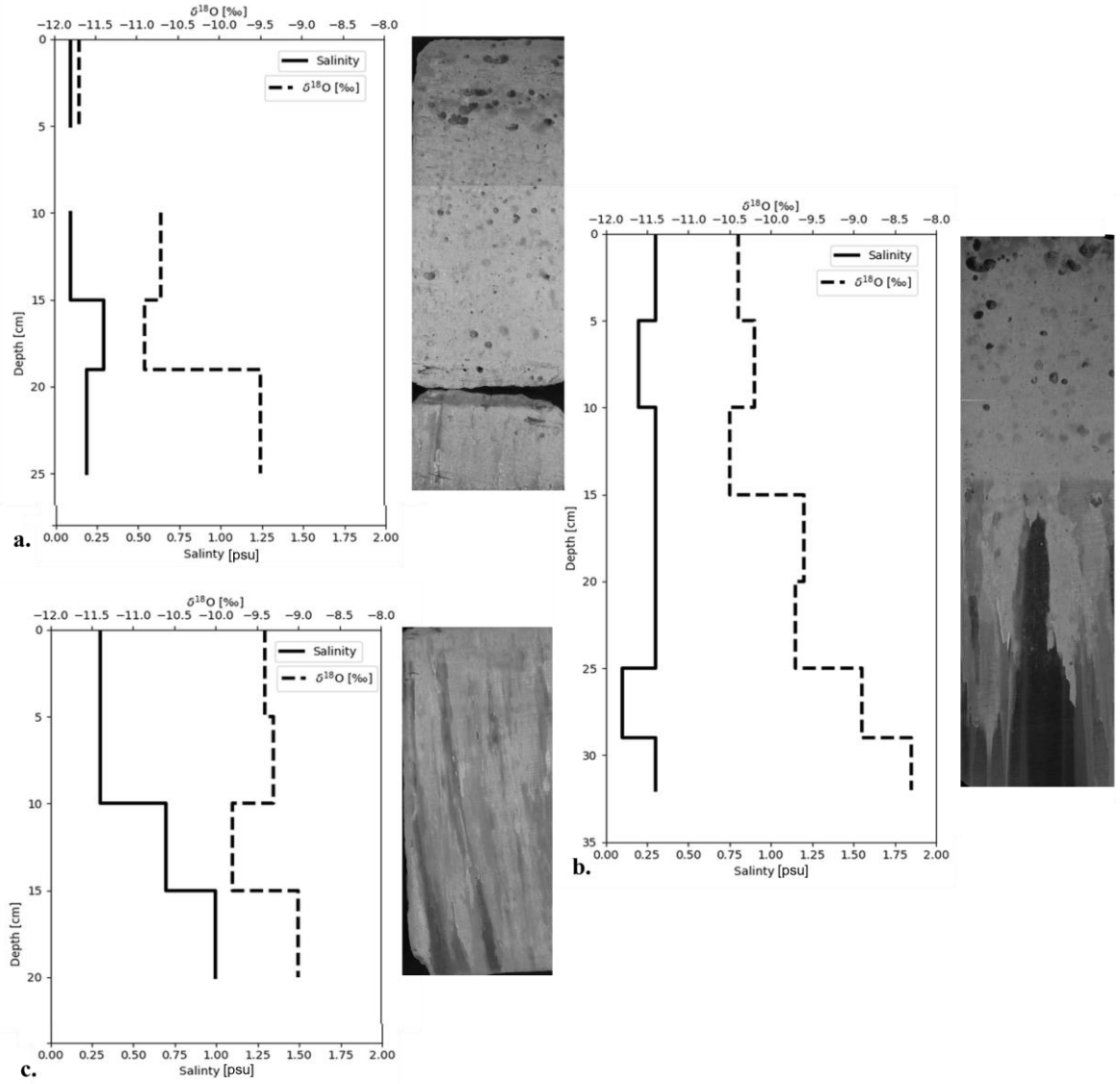

Figure 2a. Cross polarized images of ice thick sections and associated bulk ice salinity and $\delta^{18}O$ for cores gathered during the 2021 – 22 season. Location shown in Fig. 1.

All cores gathered during the 2022 – 23 seasons (Fig.2b) come from an ice cover that started to form on 25 Nov. 2022 (Table 1). Ice thickness and the amount of granular ice versus congelation ice were more consistent between the cores with all cores showing a substantial layer of granular ice, 11 to 15 cm, underlain by a layer of congelation ice from 13 to 19 cm in

thickness. At the top of the congelation ice in each core is a distinct layer having a different ice crystal orientation, appearing as a dark band. From looking at timelapse images combined with weather data, it is evident that after ice formation, there was substantial precipitation. This led to both the ice receding and flooding of the ice surface. Before snow fell, the standing water likely refroze to form a layer of superimposed ice seen at the top of the congelation layers for cores (d), (e), and (f).

Ocean salinity differed between the 2021 – 22 and 2022 – 23 seasons, from 31.5 to 31.9 psu while ocean $\delta^{18}O$ on the day of measurement was measured at -1.5 ‰ and -0.9 ‰ respectively. In addition, river water $\delta^{18}O$ was measured at -11.7 ‰ during the 2021 – 22 season and -12.1 ‰ during the 2022 – 23 season. Ocean temperature showed a clear difference between the two seasonsbeing approximately 2 °C warmer during the 2022 – 23 season. Predicted ice thickness was near to that measured being 27 cm versus 31 cm for core (d), 31 cm for core (e), and 29 for core (f). When only congelation ice is considered however, predicted ice thickness is a clear overestimation. In the 2022–23 season, snow-ice formation compensated for the insulating effect of snow. The ice cover in the 2022 – 23 season proved to be particularly resilient, withstanding periods of above freezing temperatures combined with windy, stormy conditions that had potential to cause ice breakup.

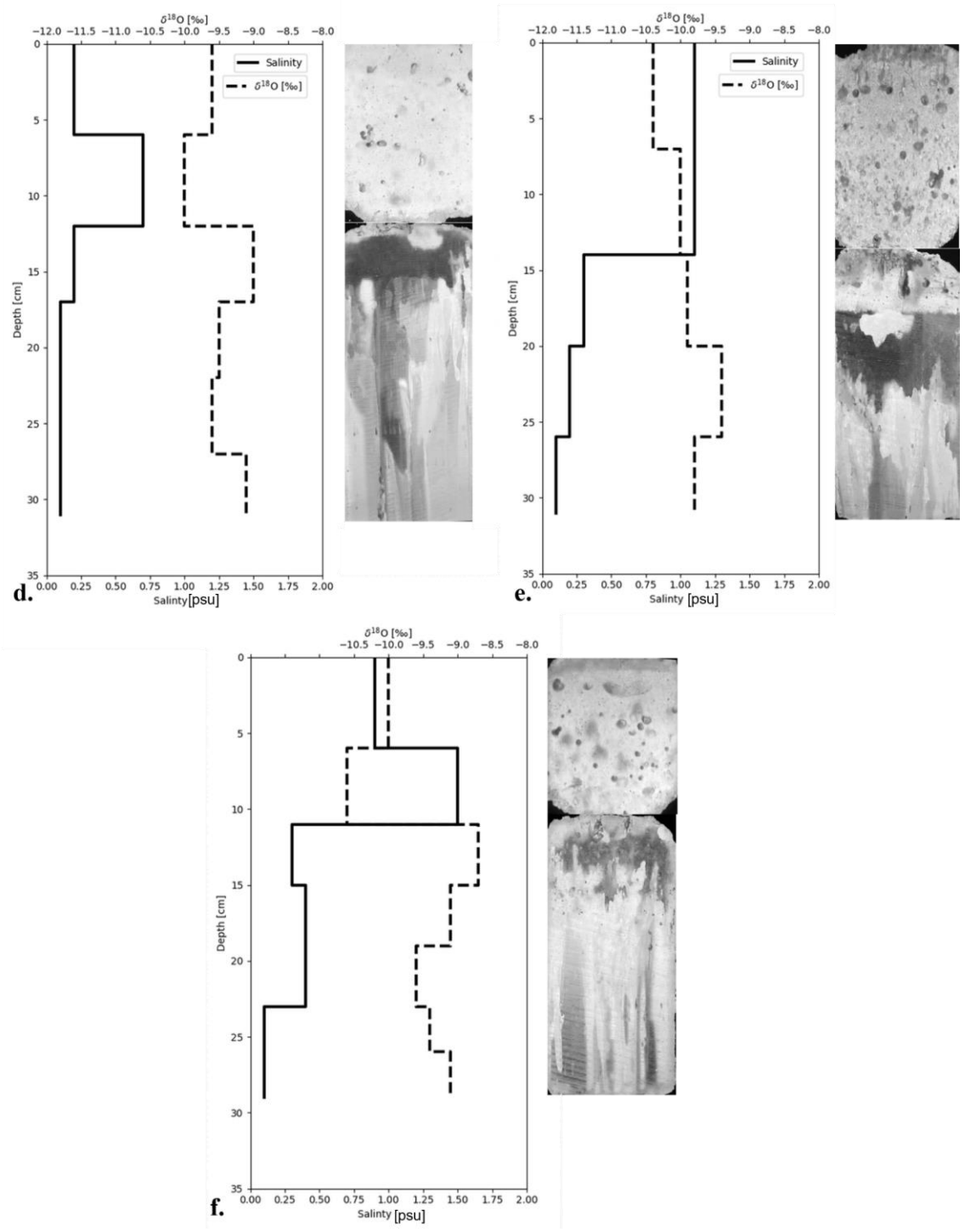

Figure 2b. Cross polarized images of ice thick sections and associated bulk ice salinity and $\delta^{18}O$ for cores gathered during the 2022 – 23 season. Location shown in Fig. 1.

Changes in weather conditions in relation to ice extent

In Fig. 3, freezing degree days from the beginning to end of the ice season are presented along with the cumulative precipitation of snow, and liquid production from rainfall and snowmelt. In O'Sadnick et al. (2022), the three seasons of ice conditions analyzed revealed ice varying in its thickness, ice type, bulk salinity and $\delta^{18}O$ signature. During the 2017 – 18

season ice was dominated by congelation growth, in 2018 – 19 ice showed a mixture of congelation and granular ice, while the third season, 2019 – 20, revealed ice entirely granular in texture, The two seasons of measurements examined here both resemble measurements from 2018 – 2019. Where they differ is in their ice formation and weather throughout the season. Both forming over a month earlier than that observed in previous seasons but experiencing different weather conditions through the ice season. In 2021 – 2022, the early season (to approximately mid-January) was dominated by subfreezing temperatures, little rainfall plus snowmelt, and relatively small additions of snow. During this time, despite subfreezing temperatures, the ice extent decreased gradually. It was not until the end of January into February after a period of increased snowfall and rainfall plus snowmelt that ice increased in extent. The fresh/brackish surface layer created by such weather presumably enabled the quick formation of new ice once subfreezing temperatures returned. Through February, temperatures remained primarily below freezing while snowfall and rainfall plus snowmelt were minimal. Ice extent held a stable position until the end of February when air temperatures began to rise consistently above freezing. A slight and shortly-lived increase in ice extent was observed on 22 March at the start of a cold period that followed almost three weeks of temperatures above or around 0 °C.

In 2022 – 2023, a substantial ice cover formed at the very beginning of the season with the maximum being reached at this time. Ice formation occurred during a unique inversion event that stretched across much of northern Norway resulting in temperatures being colder at sea level than at higher elevations. Rivers were largely unfrozen with freshwater flux presumably still higher than levels observed later in winter. Additionally, little wind was present to mix the freshwater flowing into the fjord. These factors combined to enable quick formation of a substantial ice cover in Beisfjord as well as several fjords in the region (Lange & Åsheim, 2022). Following this event, temperatures were comparatively warm throughout December into February with extended periods of time of above freezing temperatures accompanied by both snow and rainfall plus snowmelt. Ice extent gradually decreased with time lapse images showing a flooded surface. With a drop in temperature during the first week of January, a slight increase in ice extent was observed. Throughout the rest of January into February, the ice experienced a slow decrease in extent but remained present despite episodes with temperatures above freezing, rain, and snowfall. The shape of the fjord, having a small constriction about mid-way along the fjord (Fig. 1) likely assisted to keep ice in place even as it appeared to weaken along the ice front and sides. Consistent temperatures below zero were observed at the end of February and into March. Ice extent did increase during this period although not to the maximum reached before. This is likely linked to river flow being less later in winter in comparison to when ice initially formed. The ice cover disappeared during an extended period of above-zero air temperatures in April.

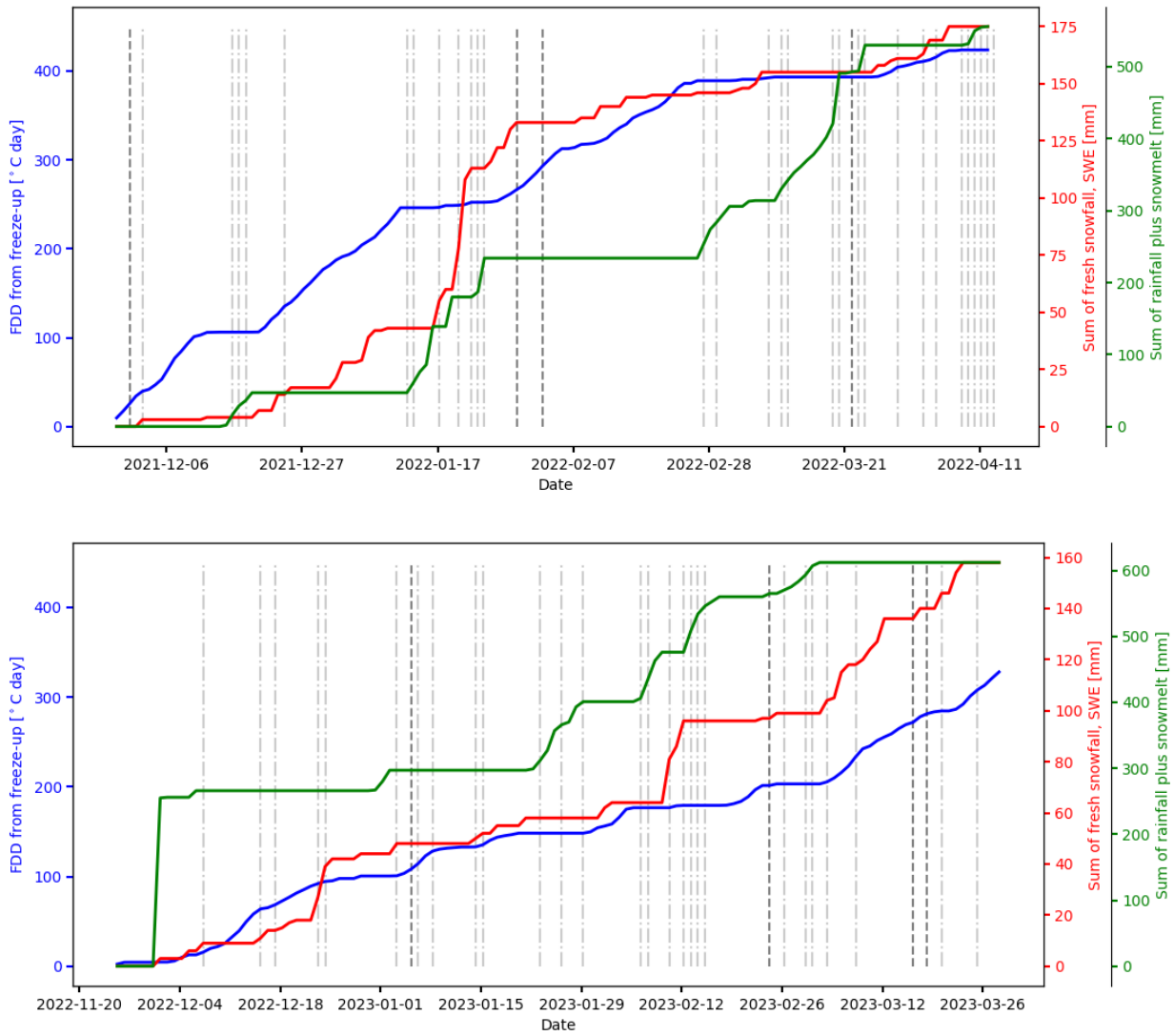

Figure 3. Freezing degree days (FDD) (blue), cumulative fresh snowfall (red), and cumulative rain plus snowmelt (green) during the ice season. Dashed lines represent decreases (light gray) and increases (dark gray) in ice extent.

CONCLUSIONS

Observations and measurements of ice conditions were gathered in Beisfjord over two winter seasons between 2021 – 23 adding to a record begun in 2017. Ice properties fell within the range observed previously, and were at the freshwater end of the scale. Ice samples displayed low values for bulk salinity and $\delta^{18}O$ with five out of the six cores being composed of both a significant layer of granular, snow ice on top of a congelation ice layer. Predictions of ice thickness differ from that measured due to insulation by snow, melt from both the top and bottom of the ice, as well as the addition of snow ice. One ice sample (core (c)) composed of only congelation ice showed good agreement with predicted ice thickness, the result likely of no snow having accumulated on the surface from the date of freeze-up to measurement combined with consistent air temperatures below freezing.

Trends in ice extent in relation to air temperature, fresh snowfall, and rainfall plus snowmelt were also examined. Ice extent showed its greatest increases during periods shortly after

precipitation or snowmelt that were followed by a decrease in air temperature. This finding is in agreement with previous work highlighting the need for a fresh or brackish water surface layer for a significant amount of fjord ice to form. During periods of little precipitation but low temperatures, ice extent tended to hold a steady position. Longer periods of above freezing temperatures, particularly in 2022 – 23, did show slow decreases in ice extent, however, the ice was able to generally hold its position until temperatures dropped below freezing again. This behavior is attributed to features along the coastline holding ice in place.

ACKNOWLEDGEMENTS

This work was partially funded by the Centre for Integrated Remote Sensing and Forecasting for Arctic Operations (CIRFA), a Centre for Research- based Innovation (Research Council of Norway project number 237906).

REFERENCES

Anderson, D. L. (1961). Growth rate of sea ice. *Journal of Glaciology*, *3*(30), 1170–1172.

Asvall, R. P. (2010). Hvordan is i vassdrag dannes – og hvordan vassdragsreguleringer påvirker isen i norske vassdrag. *Norges Vassdrags- og Energidirektorat Rapport*, *2010* (20).

Fofonoff, N., & Millard, R. (1983). Algorithms for computation of fundamental properties of seawater. *Unesco Technical Papers in Marine Science*, *44*.

Gorelick, N., Hancher, M., Dixon, M., Ilyushchenko, S., Thau, D., & Moore, R. (2017). Google Earth Engine: Planetary-scale geospatial analysis for everyone. *Remote Sensing of Environment*. https://doi.org/10.1016/j.rse.2017.06.031

Kvambekk, Å. S. (2010). Isforhold, temperatur- og saltmålinger i Holandsfjorden: Fra start på bobleanlegget i oktober 2002 til april 2008. Norges Vassdrags- og Energidirektorat Oppdragsrapport, Serie A(3).

Lange, R., & Åsheim, O. (2022, December 14). Beskyldningene har haglet etter at fjorden ble islagt: – Det må nesten ha sammenheng med strømproduksjonen. *Nordlys*.

Lussana, C., Saloranta, T., Skaugen, T., Magnusson, J., Tveito, O.E., & Andersen, J. (2018). SeNorge2 daily precipitation, an observational gridded dataset over Norway from 1957 to the present day. Earth System Science Data, 10(1), 235 – 249. https://doi.org/10.5194/essd-10-235-2018.

Norges Vassdrags- og Energidirektorat. (2019, January 14). *Nedbørfelt – REGINE*. https://temakart.nve.no/tema/nedborfelt.

O'Sadnick, M., Petrich, C., Brekke, C., Skarðhamar, J., & Kleven, Ø. (2022). Ice conditions in northern Norwegian fjords: Observations and measurements from three winter seasons, 2017–2020. *Cold Regions Science and Technology*, *204*, 103663.

O'Sadnick, M., Petrich, C., & Skarðhamar, J. (2023). Tracking changes in the fjord environment over a winter season using ice bulk salinity and δ18O. *Cold Regions Science and Technology, 208*, 103794.